INITIAL RESULTS FROM BUFFERED CRATER COUNTING FOR TWO RUPES ON MERCURY INDICATE POSSIBLE INFLUENCE FROM SECONDARY CRATERS. J. D. Gemperline[1], B. M. Hynek[1-2], S. J. Robbins[3], [1]Laboratory for Atmospheric and Space Physics & [2] Dept. of Geological Sciences, University of Colorado-Boulder, Campus Box 600 UCB, Boulder, CO 80303, [3]Southwest Research Institute, 1050 Walnut St., Suite 300, Boulder, CO 80302. john.gemperline@lasp.colorado.edu

Introduction: Orbital data from the MErcury Surface, Space ENvironment, GEochemistry, and Ranging (MESSENGER) spacecraft has confirmed that tectonic features on Mercury are globally distributed and dominantly compressional. Among these landforms are lobate scarps, of which the 30 largest such features have been termed "rupes." Rupes are observed to cross-cut all significant stratigraphic units and post-date young Calorian age smooth plains. Most efforts to constrain timing of formation for lobate scarps on Mercury have focused on cross-cutting and superpositional relationships which rely on crater counts from adjacent geologic units. Buffered crater counts (BCC) offer an alternative method for dating narrow, linear features [1] and have been used to date fluvial valley networks and tectonic features on Mars [2]. BCC allows for more accurate age determination of linear features that is independent of the surrounding terrain. To date, this method has not been used extensively on Mercury, and it has only been applied to individual thrust systems in specific regions [3-4]. Global orientations of major thrust fault systems also indicate the possibility of multi-stage deformation with the stresses related to tidal despinning peaking prior to the end of the Late Heavy Bombardment and contraction from global cooling deforming Calorian age smooth plains occurring later [5]. A comprehensive analysis of the 30 rupes imaged by MESSENGER using BCC can provide much greater temporal resolution for lobate scarp formation, and determine how many stages of compression occurred during global contraction.

Scientific Objectives: The two primary goals of this project are: (1) Analyze timing of formation of named lobate scarps, or rupes, using buffered crater counts. (2) Constrain the timing of global-scale crustal deformation of Mercury using lobate scarp ages of formation. We have begun using BCC for extensive rupes in the Rembrandt region, and plan to expand this study in the future.

Datasets: Basemaps provided by the Messenger Team include a global MDIS grayscale mosaic (250 m/pix) and MDIS color mosaic (665 m/pix) [6]. A 1 km/pix DTM exists over both Enterprise and Nautilus rupes [7] and we have generated custom DTMs using stereo pairs of NAC images. Additionally, we created controlled mosaics at 100 m/pix from ~2600 NAC images available in the PDS, filtered by incidence angle (60°-70°; 70°-80°; 80°-90°) to highlight topographic features. Crater statistics were provided from a dataset we generated of ~47,000 craters surrounding the Rembrandt region, statistically complete down to 3 km, and including craters down to ~0.5 km.

Methods: Craters were selected that intersected the area around Enterprise and Nautilus rupes. This area was determined by scarp length and antiform width. Antiform width can be approximated by dividing scarps into 50 km and measuring from scarp base to crest in the middle of each segment and averaging the measurements together for a final value. We selected the craters from our database that were superposed (post-date) on the Enterprise and Nautilus rupes and excluded obvious secondaries. Craters were binned by diameter and the weighted mean crater diameter (WMCD) for each bin was used in calculating the count area around linear features [1]. The WMCD accounts for the fact that smaller craters are more abundant than larger craters and is given by:

$$\overline{D} = \frac{\int_{D_a}^{D_b} D dN_c}{\int_{D_a}^{D_b} dN_c} = \frac{3}{2}\frac{D_a^{-2} - D_b^{-2}}{D_a^{-3} - D_b^{-3}}$$

where D_a and D_b are the smallest and largest measured crater in a bin respectively. With the WMCD for each bin the buffered area around each rupe was calculated by:

$$\text{Area} = A_{rupes} + R_{crater} * C_{rupes} + A_{crater}$$

where A_{rupes} is the area of the rupe given by length of the feature multiplied by the average antiform width, R_{crater} is crater radius, C_{rupes} is the rupe's circumference, and A_{crater} is crater area. Absolute ages were calculated from the Neukum production function for Mercury [8-9] and plotted as cumulative size-frequency distributions.

Preliminary Results: 48 post-scarp craters were mapped around Enterprise rupes and 15 post-scarp craters around Nautilus. The resulting size-frequency distributions from BCC for both Enterprise and Nautilus rupes clearly plot above the 4.0 Ga isochron [Fig 1]. Enterprise rupes visibly deforms smooth plains within the interior of Rembrandt that have been dated to ~3.7 Ga in previous work [10]. Nautilus rupes also deforms smooth plains of similar age exterior to Rembrandt basin. We used the total crater population (not just superimposed or primary craters) on the smooth plains within Rembrandt and

the resultant model age was 4.0 Ga [Fig 2]. Since deformation of the smooth plains can only occur after they are emplaced, two possibilities for the discrepancies in ages exist. (1) Determining stratigraphic relationships between craters and lobate scarps was not stringent enough, and greater discretion is needed in identifying solely superposed craters. (2) The crater population mapped via buffered crater counting in this study region is significantly influenced by secondary craters. The first explanation was investigated and we removed additional craters from the rupes buffers. This provided very similar size-frequency distributions that continued to plot above the 4.0 Ga isochron. Relatively few craters were used to date these structures, meaning reducing the number of craters further could have significant effects on the reliability of crater statistics. The second possibility could be a significant factor since secondary craters have already been noted to affect the crater population up to a diameter of ~7 km in the Rembrandt region [11]. The craters used to date rupes in this study range from 2.8-12 km in diameter, with only one crater plotted in the largest bin and thus not potentially affected by secondary craters. Since all craters larger than 12 km that intersected both scarps pre-dated scarp formation, it is not possible to discern from this data where secondary craters begin to play a role. However, this could have important implications for future mapping efforts and studies on Mercury relying on relatively small areas for crater statistics (< 10^5 km^2) or specialized methods such as buffered crater counting.

Future Work: A less stringent approach to BCC takes into effect craters with ejecta blankets that intersect the linear feature of interest. This produces a wider buffer area for crater counting and could potentially improve crater statistics and include larger diameter craters outside the size where secondary craters are a significant factor. Including crater ejecta also comes with greater difficulty and subjectivity in determining stratigraphic relationships, since many ejecta blankets on relatively young craters on Mercury have been obliterated. Another way to potentially include larger count areas is by conducting BCCs around thrust fault systems as opposed to individual features. Future age determinations will also employ the newer model production functions as well as the Neukum production function.

Acknowledgements: Funding for this work came from NASA PGG grant NNX14AP51G.

References: [1] Tanaka, K.L. (1982) *NASA TM-85127*, 123–125. [2] Hoke, M.R.T. & B.M. Hynek (2009) *JGR, 114*. [3] Galluzzi, V. et al., (2015) *EPSC, 10*, abstract #927. [4] Giacomini, L. et al., (2015) *Geol. Soc. S.P., 401*, 291-311. [5] Watters, T.R., et al., (2015) *Geophys. Res. Lett., 42*, 3755-3763. [6] http://messenger.jhuapl.edu/the_mission/mosaics.html. [7] Preusker, F.J. et al., (2011) *PSS, 59*, 1910–1917. [8] Neukum, G. et al., (2001a) *ISSI Proc., 2000*, 55-86. [9] Neukum, G. et al., (2001b) *Planet. Space Sci. 49*, 1507-1521. [10] Ferrari, S. et al., (2015) *Geol. Soc., London, Spec. Pubs.* 401.1: 159-172. [11] Chapman, C.R. et al., (2010) *Meteorit. Soc, 73*, abstract #5325. [12] Michael G.G., Neukum G., (2010) *Earth Planet. Sc Lett, 294*, 223-229.

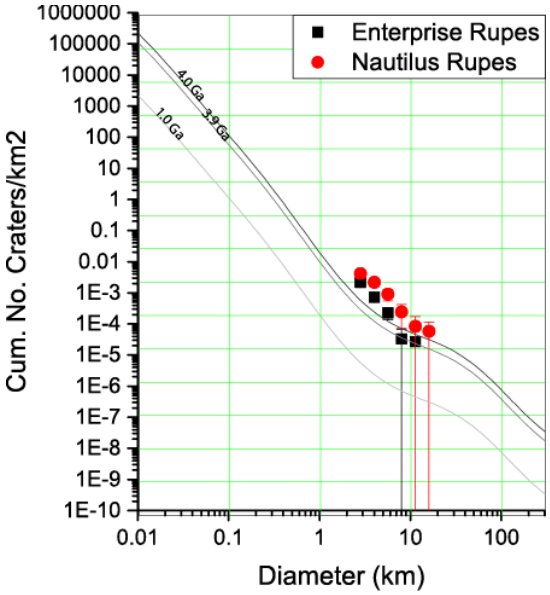

Fig. 1: Cumulative size-frequency distribution plot of post-dating craters around Enterprise and Nautilus rupes with isochrones from the NPF.

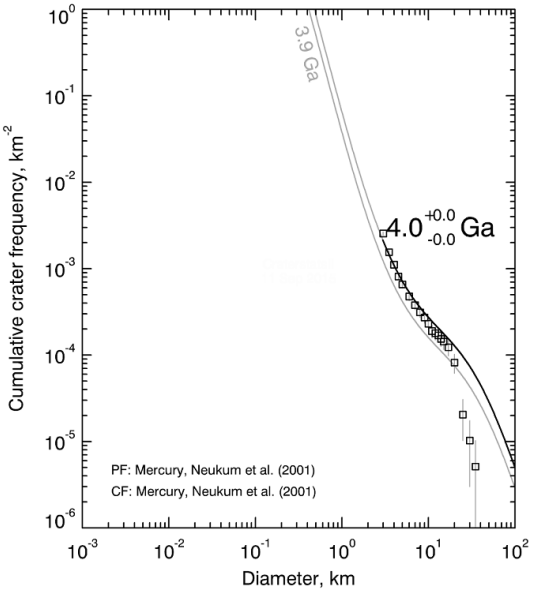

Fig. 1: Cumulative size-frequency distribution of all craters located on the smooth plains within Rembrandt basin plotted in Craterstats [12].